Journal of Additive Manufacturing Technologies
DOI: 10.18416/JAMTECH.2212695

Infinite Science | Publishing

Energy density determination for L-PBFP of Ti-6Al-4V alloy for various beam diameters and hatch distances

M. Mollamahmutoğlu[1*], O. Yılmaz[1], C. Köseoğlu[2], H. Tecer[2], F. Özaydın[2], Ö. F. Kocaoğlu[3], and E. Z. Emir[3]

[1] *Advanced Manufacturing Technologies Research Group (AMTRG), Gazi University, Ankara, Türkiye*
[2] *ESTAŞ, Şeyh Şamil OSB Mah. Halis Vermezoğlu Cd. No:57, Sivas, Türkiye*
[3] *digiMODE, Alınteri Bulvarı, No: 52 Ostim 06374, Yenimahalle, Ankara, Türkiye*
[*] *Corresponding author, email: mehmetmollamahmutoglu@gmail.com*

Abstract

It is important to determine the appropriate energy densities to achieve an ideal (defect-free) production in the laser powder bed fusion process. In this study, energy density levels for Ti-6Al-4V alloy were determined through simulations with a model using a dynamic volumetric heat source. Undesirable situations such as fusion problems, balling, excessive evaporation, and keyhole regime are accepted as criteria for the evaluation. The developed process window covers analysis for different beam diameters of 50, 80, and 100 micrometers, and hatch distances ranging from 30 to 100 micrometers. Laser power and laser scan speed range from 50 to 200 W and 250 to 1500 mm/s, respectively. The results have shown that higher laser power with low scan speed causes high evaporation and keyhole formation. On the other hand, unstable melt-pools, fusion problems and balling may be encountered for lower laser power with high scan speed. Consequently, the analysis results are to be used as a guide before further experimental tests.

Keywords: Laser powder bed fusion process, Additive manufacturing, Process window.

© 2022 M. Mollamahmutoğlu; licensee Infinite Science Publishing

This is an Open Access article distributed under the terms of the Creative Commons Attribution License (http://creativecommons.org/licenses/by/4.0), which permits unrestricted use, distribution, and reproduction in any medium, provided the original work is properly cited.

1. Introduction

In the laser powder bed fusion process (L-PBFP), parameter selection is highly crucial in terms of manufactured part quality [1]. Parts with good tolerances and mechanical properties as well as minimum metallurgical problems can be produced with the selection of appropriate parameters. For this purpose, the energy density must be sufficient to provide the desired fusion between hatches and between layers. Otherwise, the porosity caused by fusion problems reduces the quality of the produced part. Balling may occur as a further situation [2], especially in the case of interlayer fusion problems. On the other hand, excessive energy input means the waste of material and energy. Because high energy may cause high evaporation. As a result, evaporation-induced porosity is encountered in the produced part. In an extreme case, the keyhole regime may also occur, which significantly increases the pore size. In this case, just as with insufficient energy, the quality of the part decreases.

In this study, a numerical study was done for critical process parameters to be tested in future experimental work. A model, which includes a dynamic volumetric heat source [3], has been constructed in COMSOL Multiphysics® software, and simulations were performed. The suitability of the parameter sets consisting of various beam diameters, laser powers, scan speeds, and hatch distances for Ti-6Al-4V alloy was investigated in detail.

2. Material and methods

The parameter sets for the experiment, which will be conducted in the workshop tests, are determined via the DOE method and are given in Table 1. Here, beam diameter (50, 80, 100 µm), laser power (50-200 W), scan speed (250-1500 mm/s), and hatch distance (30-100 µm) were taken as input parameters. Other assumptions related to the process conditions are summarized in Table 2.

Different criteria are taken into account to determine whether a parameter is suitable for production. The parameter used for criteria here are as follows: melt pool shape and dimensions, average temperature, and interlayer and interscan fusion sufficiencies. The Bowl type is accepted as the most suitable melt pool shape. In addition, even if the profile is suitable, it is not desirable for the melt pool dimensions to be larger than necessary. For bonding sufficiency between layers, the melt pool depth to powder layer thickness ratio is supposed to be at least 1.5 as the criterion. However, not exceeding 3 is accepted as another criterion [4, 5]. For interscan sufficiency, there must not be unmelted areas between scans. Lastly, it is desirable that the average pool temperature is far from the alloy boiling point. Consequently, it has been checked whether the outputs obtained from the simulations meet the criteria given above. Thus, a process window is revealed for the investigated beam diameters.

Table 1. Parameter sets used in simulations.

	Set no.	Laser power (W)	Scan speed (mm/s)	Hatch distance (µm)
Beam diameter 100 (µm)	1	100	500	85
	2	200	500	85
	3	100	1400	85
	4	200	1400	85
	5	100	950	70
	6	200	950	70
	7	100	950	100
	8	200	950	100
	9	150	500	70
	10	150	1400	70
	11	150	500	100
	12	150	1400	100
	13	150	950	85
Beam diameter 80 (µm)	1	100	500	65
	2	200	500	65
	3	100	1500	65
	4	200	1500	65
	5	100	1000	50
	6	200	1000	50
	7	100	1000	80
	8	200	1000	80
	9	150	500	50
	10	150	1500	50
	11	150	500	80
	12	150	1500	80
	13	150	1000	65
Beam diameter 50 (µm)	1	50	250	40
	2	150	250	40
	3	50	1400	40
	4	150	1400	40
	5	50	825	30
	6	150	825	30
	7	50	825	50
	8	150	825	50
	9	100	250	30
	10	100	1400	30
	11	100	250	50
	12	100	1400	50
	13	100	825	40

In addition to the volumetric heat source, powder-bulk transformation (via thermal hysteresis), radiation and convection heat losses at the boundaries were evaluated in the model. The following empirical expression was used for the heat source efficiency for different beam diameters in Ti-6Al-4V alloy [6]:

$$\alpha_{Ti-6Al-4V} = \alpha_1 + \alpha_2 / \left[1 + e^{-\left(\frac{V-V_0}{C}\right)}\right] \quad (1)$$

And the relevant parameters in the equation are as follows:

$$\alpha_1 = 0.2327 + \frac{0.201}{1+e^{-\left(\frac{P(100/D)^{\pi/2} - 114.4438}{28.281}\right)}}$$

$$\alpha_2 = 0.4424 + \frac{-0.5679}{1+e^{-\left(\frac{P(100/D)^{\pi/2} - 153.3912}{-13.2179}\right)}}$$

$$C = -0.1748 + \frac{0.4684}{1+e^{-\left(\frac{P(100/D)^{\pi/2} - 116.8547}{-25.7217}\right)}}$$

$$V_0 = 0.7173 + \frac{0.1275}{1+e^{-\left(\frac{P(100/D)^{\pi/2} - 154.6248}{-2.444}\right)}}$$

Here α_1 and α_2 are the efficiency coefficients. V_0 and C are the scan speed coefficients. P and D are laser power and beam diameter, respectively. More detailed information on the model used, governing equations, and boundary conditions can be found in the relevant references [6, 7].

Table 2. Some assumptions related to the conditions.

Beam diameter	(1/e²- Gaussian)
Substrate temperature	20 °C
Scan length	2 mm
Scan strategy	Unidirectional
Powder layer thickness	30 µm
Powder packing density	0.5

3. Results and discussion

Laser efficiency values are calculated according to (1) and presented in Fig. 1. Here, efficiency means the net energy input to the material other than evaporation, including absorption. This value, which is around 0.3-0.4 for Ti-6Al-4V under normal conditions, may decrease due to the spattering, denudation, and laser plume instability. On the other hand, it can increase significantly due to the deformation of the liquid metal surface. In particular, keyhole formation can cause the absorption of most of the incoming laser energy [8-10].

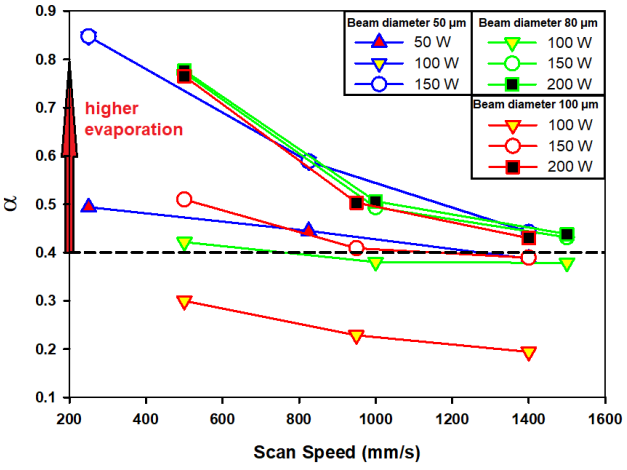

Fig 1. Laser absorption/efficiency values for parameter sets

As shown in Fig. 1, an increase above 0.4 means that the evaporation has increased enough to push the liquid metal mass. This situation also means unexpected

energy input rise. The limit for this rise depends on the balance between the energy loss due to evaporation and the energy gain due to surface deformation as a result of evaporation [11]. Although this nonlinear behavior seems advantageous at first, it is not desired due to the material waste and porosity problem. Therefore, as a general principle, high energy densities (high laser energy /small beam diameter/low scan speed) should be avoided.

In Table 3, the melt pool depths to powder layer thickness ratios are given. In fact, this ratio can change with the heat accumulation in the upper layers and the differentiation of the actual powder layer thickness from the nominal value. Considering the powder packing density, the actual powder layer thickness can be twice the nominal value. However, it would approach the nominal value during melting and densification. Therefore, a ratio of one and a half can be considered as the minimum criterion. Increasing this ratio above 3 is unnecessary in terms of energy use. Secondly, an increase in this ratio to 3 indicates high evaporation. The exception to this situation may be the formation of a liquid metal lake by applying a low energy density to a region for a long time. In this way, penetration can be increased while keeping evaporation low. However, in this case, the melt pool width would also increase significantly. This situation could affect dimension tolerance and surface roughness.

Table 3. Melt pool depth to powder layer thickness ratios for different beam diameters.

Set no.	100 µm	80 µm	50 µm
1	1.5	2	2
2	6	4	5
3	<1	<1	<1
4	1.5-2	2	1.5-2
5	<1	1.5	1
6	2.5-3	2-2.5	2.5
7	<1	1.5	1
8	2.5-3	2-2.5	2.5
9	3-3.5	3-3.5	4
10	1.5	1.5	1-1.5
11	3-3.5	3.5	4
12	1.5	1.5	1-1.5
13	1.5-2	1.5-2	2.5

Fig. 2 presents the process window for a beam diameter of 50 micrometers. Here, suitable parameters are colored green, and unsuitable ones are colored red. Hatch distance is expressed by symbol size. Some profiles have been calculated to have a large bowl. But these are not ideal. Because they are both deep and wide pools where evaporation is extremely high. The reason why they are not in the keyhole formation is that the width is also large. A smaller beam diameter can enable production with higher precision tolerances. However, in general, low energy and scan speed may be preferred to keep evaporation low. In addition, hatch distances are generally expected to be small. Therefore, production times are relatively longer. In short, it becomes pointless to use small beam diameters for parts that do not require high dimensional tolerances.

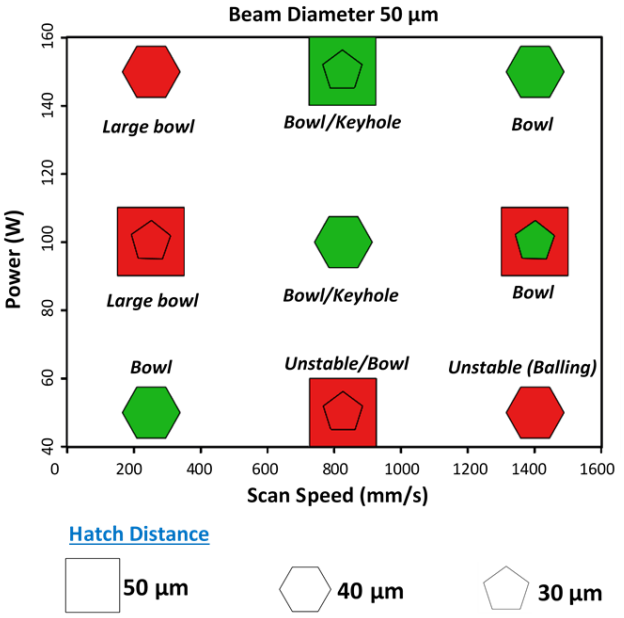

Fig 2. Process window for 50 µm beam diameter.

Fig. 3 shows the process window for a beam diameter of 80 micrometers. With the increase in beam diameter, higher laser energies have become available. However, low laser energy levels, where conditions such as unstable pools and balling occur, have also shifted. At low energy levels such as 100 W-1000 mm/s, particular attention should be paid to the hatch distance. Because at these energy levels, fusion with the sublayer could be achieved at minimum criteria. Thus, hatch distance should be reduced to avoid porosity.

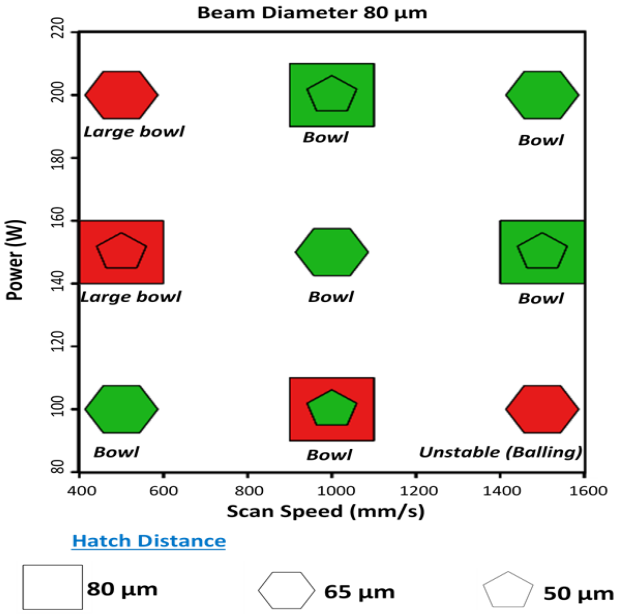

Fig 3. Process window for 80 µm beam diameter.

The process window for a beam diameter of 100 micrometers is presented in Fig 4. As can be seen, the use of low energy levels has become even more limited.

In these cases, fusion with the sublayer can only be achieved at low scan speeds. As it can be understood, the powder layer thickness is a very important parameter that determines the laser energy and scan speed ranges. In order to make different beam diameters and energy densities suitable for a material, first of all, changing the powder layer thickness should be considered. Because laser power increase also brings evaporation. Increasing the scan speed does not always help in such a situation. Because the material also has limits in terms of the transfer of heat from the upper surface. Even if keyhole formation does not occur, unstable laser plumes may occur as a result of evaporation and smoke.

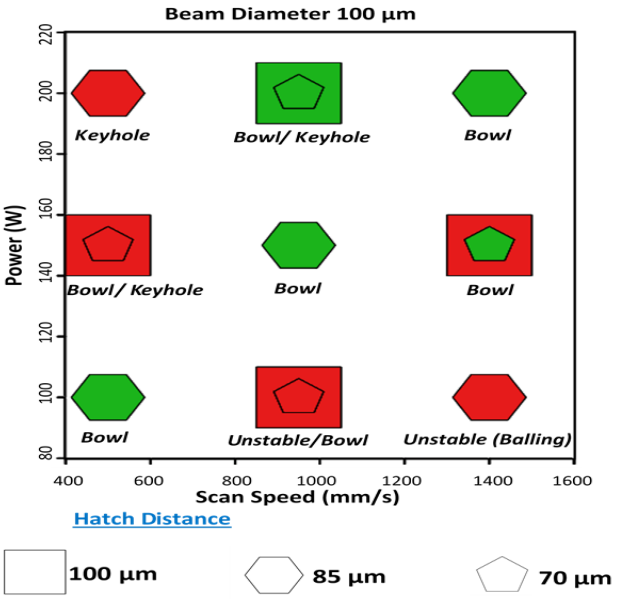

Fig 4. Process window for 100 µm beam diameter.

Adjusting the hatch distance is functional in cases where there is a lack of fusion between scans. As an example, snapshots from a simulation are presented in Fig. 5. As can be seen, the hatch distance of 100 micrometers is large for the parameter of 150 W-1400 mm/s. In the figure, the temperature distribution in subfigure a and the molten region (dark red) in subfigure b are shown. Although the energy density is sufficient for fusion with the sublayer, problematic areas are seen due to the large hatch distance. From the front profile perspective in subfigure c, it can be observed that the fusion problems increase towards the interlayer border, and this situation indicates fusion-induced porosity. In such a case, reducing the hatch distance solved the problem for the same parameter.

Reducing the hatch distance can be of little help in cases where there is a lack of fusion with the sublayer. Scan length also plays a role here. In other words, when the laser beam will pass is as important as how far from the same point it will pass. In any case, an extremely short hatch distance approach would greatly increase the production time and would become a kind of remelting or reheating process. Such an approach could be considered for a purpose such as microstructural change or stress relief rather than solving fusion problems [12].

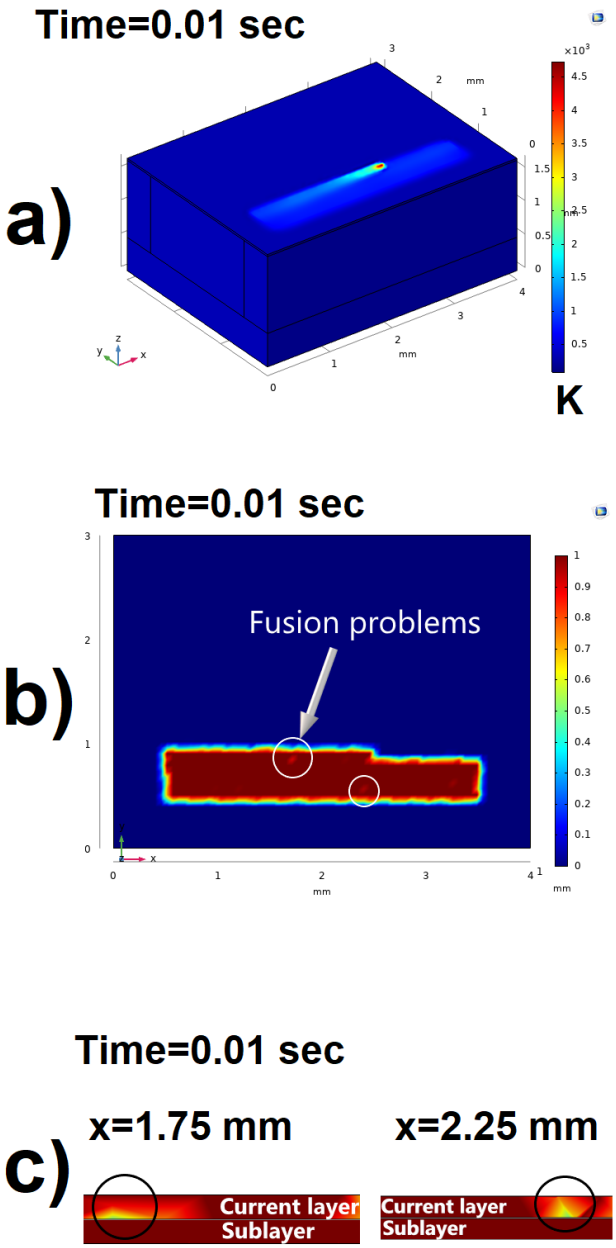

Fig 5. 150 W-1400 mm/s, 100 µm beam diameter, a) Temperature distribution, b) Top view melted region, fusion problems, c) Front profiles melted region, fusion problems at x=1.75 and x=2.25.

The suitability of the energy densities obtained is presented in Fig. 6. Here, the energy density is defined as:

$$E = \frac{P}{Vh} \tag{2}$$

Where P, V, and h are laser power, scan speed, and hatch distance, respectively. The appropriate energy densities are marked in green in the figure. These energy densities have been determined according to the criteria specified previously and indicate suitability in terms of production. It is possible to get a rough idea in

terms of suitable energy density fields. Thus, the area containing possible suitable energy densities for intermediate beam diameter sizes appears. In the figure, this region, along with the high and low energy density regions, is roughly shown with dashed lines.

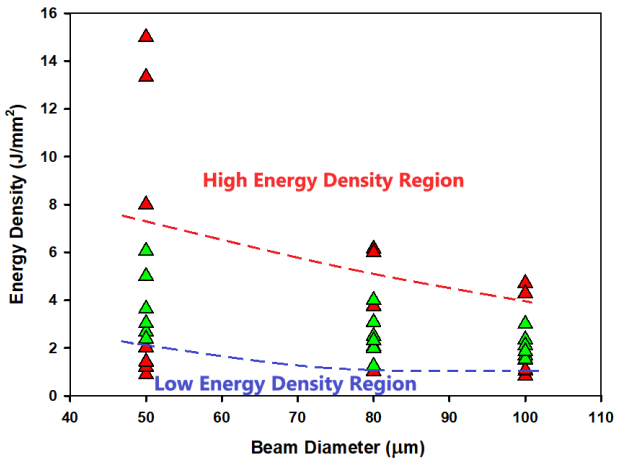

Fig 6. Ideal energy densities for various beam diameters.

4. Conclusions

In this study, a process window generation procedure for Ti-6Al-4V alloy, which considers various process parameters, is presented and can be applied to other alloys in L-PBFP. The result of the study can be summarized as follows:

- The beam diameter is the most dominant parameter in the selection of the ideal hatch distance.
- The ideal penetration (melt pool) depth is approximately 1.5 to 2.5 times the powder layer thickness.
- In addition to the thermo-physical properties of the material used, the powder layer thickness also limits the usable beam diameter and laser power range.
- Reducing the energy density by means of scan speed cannot compensate for the increase in laser energy after a certain point. Here, the limits on the energy transfer ability of the material should also be considered.

Acknowledgments

None

Author's statement

Conflict of interest: Authors state no conflict of interest. Informed consent: Informed consent has been obtained from all individuals included in this study.

Ethical approval: The research related to human use complies with all the relevant national regulations, institutional policies and was performed in accordance with the tenets of the Helsinki Declaration, and has been approved by the authors' institutional review board or equivalent committee.

References

1. Oliveira, J. P., et al, Processing parameters in laser powder bed fusion metal additive manufacturing, Materials and Design, 2020. 193, 108762.
2. Boutaous, M., et al, Balling phenomenon in metallic laser based 3D printing process, International Journal of Thermal Sciences, 2021. 167, 107011
3. Mollamahmutoglu, M. and Yılmaz, O., Volumetric Heat Source Model for Laser-Based Powder Bed Fusion Process in Additive Manufacturing. Thermal Science and Engineering Progress, 2021. 25, 101021.
4. Gong H., et al, Melt Pool Characterization for Selective Laser Melting of Ti-6Al-4V Pre-alloyed Powder. 2014 International Solid Freeform Fabrication Symposium, 2014.
5. Dilip, J. J., et al, Influence of processing parameters on the evolution of Melt Pool, porosity, and microstructures in ti-6al-4v alloy parts fabricated by selective laser melting. Progress in Additive Manufacturing, 2017. 2, 157–167.
6. Yildiz, A. K., et al, Computational Evaluation of Temperature-Dependent Microstructural Transformations of Ti6Al4V for Laser Powder Bed Fusion Process. Journal Of Materials Engineering and Performance, 2022. 31, 7191–7203.
7. Yıldız, A. K., et al, A numerical investigation of the effect of support thickness and void ratio on thermal behavior and possible martensite decomposition in laser powder-bed fusion process. Journal of Additive Manufacturing Technologies, 2021. 1,549–549.
8. Fabbro, R., et al, Gunenthiram, V., Analysis and possible estimation of keyhole depths evolution, using laser operating parameters and material properties. Journal of Laser Applications, 2018. 30, 032410.
9. Ye, J. et al, Energy coupling mechanisms and scaling behavior associated with laser powder bed fusion additive manufacturing. Advanced Engineering Materials, 2019. 21, 1900185.
10. Ye, J. et al, Laser absorption and scaling behavior in powder bed fusion additive manufacturing of metals. Conference on Lasers and Electro-Optics, 2018.
11. Fabbro, R., Depth dependence and keyhole stability at threshold, for different laser welding regimes. Applied Sciences, 2020. 10, 1487.
12. Barriobero-Vila, P. et al, Inducing Stable α + β Microstructures during Selective Laser Melting of Ti-6Al-4V Using Intensified Intrinsic Heat Treatments. Materials, 2017. 10, 268.